Weierstraß-Institut
für Angewandte Analysis und Stochastik
Leibniz-Institut im Forschungsverbund Berlin e. V.

Preprint ISSN 2198-5855

Hybrid finite-volume/finite-element schemes for $p(x)$-Laplace thermistor models

Jürgen Fuhrmann, Annegret Glitzky, Matthias Liero

submitted: March 3, 2017

Weierstrass Institute
Mohrenstraße 39
10117 Berlin
Germany
E-Mail: juergen.fuhrmann@wias-berlin.de
annegret.glitzky@wias-berlin.de
matthias.liero@wias-berlin.de

No. 2378
Berlin 2017

2010 *Mathematics Subject Classification.* 65M08, 35J92, 35G60, 35Q79, 80M12, 80A20.

Key words and phrases. Finite volume scheme, $p(x)$-Laplace thermistor model, path following.

Acknowledgments. A.G. and M.L. gratefully acknowledge the funding received via Research Center MATHEON supported by the Einstein Foundation Berlin within project SE2.

Edited by
Weierstraß-Institut für Angewandte Analysis und Stochastik (WIAS)
Leibniz-Institut im Forschungsverbund Berlin e. V.
Mohrenstraße 39
10117 Berlin
Germany

Fax: +49 30 20372-303
E-Mail: preprint@wias-berlin.de
World Wide Web: http://www.wias-berlin.de/

Hybrid finite-volume/finite-element schemes for $p(x)$-Laplace thermistor models

Jürgen Fuhrmann, Annegret Glitzky, Matthias Liero

Abstract

We introduce an empirical PDE model for the electrothermal description of organic semiconductor devices by means of current and heat flow. The current flow equation is of $p(x)$-Laplace type, where the piecewise constant exponent $p(x)$ takes the non-Ohmic behavior of the organic layers into account. Moreover, the electrical conductivity contains an Arrhenius-type temperature law. We present a hybrid finite-volume/finite-element discretization scheme for the coupled system, discuss a favorite discretization of the $p(x)$-Laplacian at hetero interfaces, and explain how path following methods are applied to simulate S-shaped current-voltage relations resulting from the interplay of self-heating and heat flow.

1 Introduction

Presently, carbon-based semiconductors are used in smartphone displays and increasingly in TV screens. Due to the fascinating properties of organic light-emitting diodes (OLEDs), e.g. large-area surface emission, semi-transparency, flexibility, also lighting applications are of great interest. However, lighting requires a much higher brightness than displays and hence higher currents are necessary. These cause substantial Joule self-heating accompanied by unpleasant brightness inhomogeneities of the panels. An appropriate simulation tool for the electrothermal description of OLEDs can help to validate cost-efficient device concepts by accounting for nonlinear self-heating effects.

Applying a voltage to an organic semiconductor device induces a current flow which leads to a power dissipation by Joule heating and hence also a temperature rise. As higher temperatures improve the electrical conductivity in organic materials, higher currents occur. Thus, a positive feedback loop develops that either leads to the destruction of the device by thermal runaway if the generated heat cannot be dispersed into the environment or results in S-shaped current-voltage characteristics. In particular, in the latter case regions of negative differential resistance (S-NDR) appear, where currents increase despite of decreasing voltages, see Fig. 1 (right). Devices that show such an electrothermal interplay are called thermistors.

S-NDR has been verified for the organic material C_{60} in [7] and for organic materials used in OLEDs in [6], where the temperature dependence of the conductivity is modeled by an exponential law of Arrhenius type, which features an activation energy that is linked to the energetic disorder in the organic material. Due to the huge aspect ratios of OLED panels, such devices cannot be regarded as a single spatially homogeneous thermistor device, but rather as an array of thermally and electrically coupled thermistor devices. In particular, the self-heating, and hence also the local differential resistance, is now a collective property of neighboring thermistors. One attempt is followed in [6] where the electrothermal behavior of OLEDs is investigated by means of electrically and thermally coupled thermistor networks and SPICE simulations.

In this paper, we present a mathematical model for the current and heat flow in organic semiconductor devices consisting of a coupled PDE system for the electrostatic potential and the temperature, see

DOI 10.20347/WIAS.PREPRINT.2378 Berlin 2017

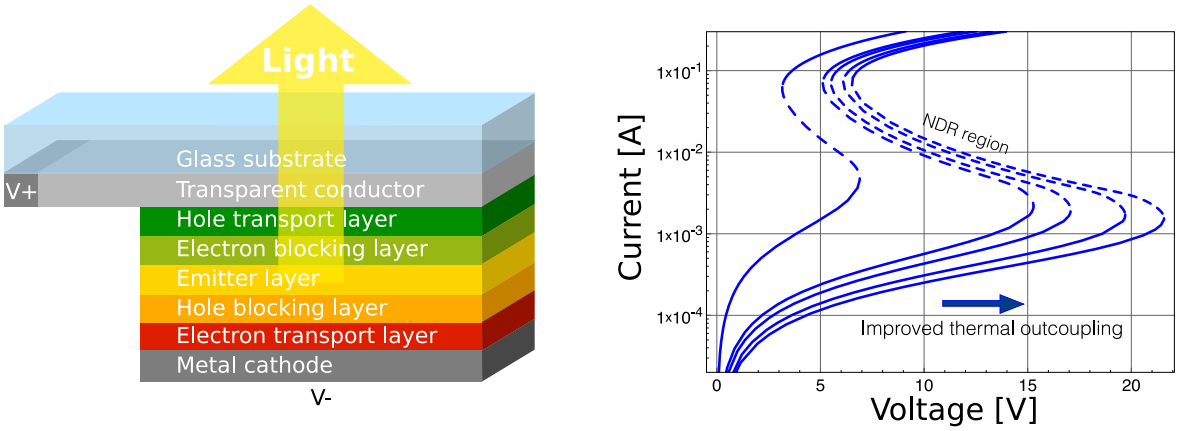

Figure 1: Schematic view of an OLED stack (left) and simulated current-voltage characteristics for different thermal outcoupling regimes, regions of negative differential resistance are dashed (right)

Sect. 2. This PDE modeling approach gives much more flexibility concerning variations in geometry and material composition than network models. An essential feature of our PDE model is that the current flow equation is of $p(x)$-Laplace type, where the exponent $p(x)$ takes the non-Ohmic behavior of the organic layers into account. The exponent is in general discontinuous but piecewise constant as the different functional layers exhibit different power laws. In Sect. 3 we introduce a numerical scheme for the simulation of current and heat flow in OLEDs. One of the major challenges is the derivation of a stable scheme for the $p(x)$-Laplacian, which we address by using a hybrid finite-volume/finite-element approach which is discussed in Sect. 4. Whereas the presented scheme preserves lower bounds for the temperature, a convergence proof is still under discussion. Challenges arise from bad analytical properties of the Joule heat term. Finally, in Sect. 5 we describe a path following method which enables us to simulate the electrothermal behavior of organic semiconductor devices also in the S-NDR regime.

2 PDE Modeling of Current and Heat Flow

To describe the interplay of current and heat flow in OLEDs the following empirical PDE model was developed in [9]. It consists of the current flow equation for the electrostatic potential φ and the heat equation for the temperature T

$$\begin{aligned} -\nabla \cdot S(x,T,\nabla\varphi) &= 0, \\ -\nabla \cdot \big(\lambda(x)\nabla T\big) &= H(x,T,\nabla\varphi) \end{aligned} \qquad \text{on } \Omega \subset \mathbb{R}^d \tag{2.1}$$

with electrical current density S, heat conductivity λ, and Joule heat term H. The special features of the model are the Arrhenius-like temperature law as well as the non-Ohmic current-voltage relations incorporated by a power law in the function S,

$$S(x,T,\nabla\varphi) = \kappa_0(x)F(x,T)|\nabla\varphi|^{p(x)-2}\nabla\varphi, \quad F(x,T) = \exp\Big[-\frac{E_{\mathrm{act}}(x)}{k_{\mathrm{B}}}\Big(\frac{1}{T}-\frac{1}{T_a}\Big)\Big].$$

Here, $T_a > 0$ and k_{B} denote the fixed ambient temperature and Boltzmann's constant. The quantitites κ_0, p, and E_{act} are material dependent effective conductivity, power law exponent, and activation energy, respectively, which have to be extracted from measurements. The first equation in (2.1) becomes of $p(x)$-Laplacian type with discontinuous but piecewise constant exponent p. In particular, we have $p(x) \equiv 2$ in Ohmic materials such as electrodes and different values $p(x) > 2$ in organic layers. The Joule heat term in the second equation of (2.1) takes the form

$$H(x, T, \nabla\varphi) = \eta(x, T, \nabla\varphi)\kappa_0(x)F(x, T)|\nabla\varphi|^{p(x)},$$

where $\eta(x, T, \nabla\varphi) \in [0, 1]$ represents the light-outcoupling factor. The system is complemented by Dirichlet and no-flux boundary conditions for the potential φ at the contacts Γ_D and the insulating parts Γ_N of the boundary, and Robin boundary conditions for the heat flow to describe the coupling to the environment

$$\begin{aligned} &\varphi = \varphi^D \text{ on } \Gamma_D, \qquad S(x, T, \nabla\varphi) \cdot \nu = 0 \text{ on } \Gamma_N, \\ &-\lambda(x)\nabla T \cdot \nu = \gamma(x)(T - T_a) \text{ on } \Gamma = \partial\Omega. \end{aligned} \tag{2.2}$$

Since the Joule heat term H is a priori only in L^1, the mathematical treatment of the system is not straightforward. For analytical results concerning the existence, boundedness and regularity of solutions to Problem (2.1), (2.2) we refer to [3, 4, 8].

3 Numerical Scheme

Since we have to deal with piecewise constant functions $p(x)$, we subdivide the computational domain $\overline{\Omega} = \bigcup_{r\in\mathcal{R}} \overline{\Omega}_r$ into disjoint subdomains coinciding with the regions of continuity of the coefficients. We call the surface between two neighboring regions *hetero interface*. Due to its ability to preserve the maximum principle of the current flow equation and the positivity of the temperature, we prefer a two-point flux finite-volume method for the dicretization of (2.1), (2.2) over methods defined on more general meshes (e.g. [5]). Our control volumes are Voronoi cells based on a grid with the boundary conforming Delaunay property with respect to boundaries and hetero interfaces [11]. Let $\mathcal{V}$ denote the set of Voronoi boxes and $m = \#\mathcal{V}$ be the number of cells. We assume that each control volume $K \in \mathcal{V}$ contains a collocation point $x_K \in \overline{\Omega}$.

Let $K \in \mathcal{V}$ be an internal Voronoi box meaning that $\mathrm{mes}_{d-1}(\overline{K} \cap \overline{\partial\Omega}) = 0$. We apply Gauss's theorem to the integral of the flux divergence to obtain for the current flow equation in (2.1) the flux balance with further subdivision into contributions from adjacent subdomains ($\kappa_{0,r}$ and F_r indicate the corresponding values in region Ω_r):

$$0 = \int_K \nabla \cdot S(x, T, \nabla\varphi)\,\mathrm{d}x = \sum_{r\in\mathcal{R}} \sum_{L\sim K} \int_{\overline{K}\cap\overline{L}\cap\Omega_r} \kappa_{0,r}\, F_r(T)|\nabla\varphi|^{p_r-2}\nabla\varphi \cdot \nu_{KL}\,\mathrm{da}, \tag{3.1}$$

where $L \sim K$ indicates that L is adjacent to K and ν_{KL} is the unit normal vector pointing from K into L. Note that the normal flux over a surface $\overline{K} \cap \overline{L} \cap \Omega_r$ does not only depend on the normal components of $\nabla\varphi$ but on the modulus of the full gradient. To take this into account we compute the approximation of $|\nabla\varphi|^2$ on $\overline{K} \cap \overline{L} \cap \Omega_r$ as the average squared norms of the P1 finite element

gradients $\nabla_\tau\varphi$ over the set $\mathcal{T}_{K,L,r}$ of all simplices τ (triangles in 2D) in the underlying Delaunay triangulation adjacent to the edge $\overline{x_K x_L}$ and belonging to Ω_r:

$$\big|\nabla\varphi\big|^2|_{\overline{K}\cap\overline{L}\cap\Omega_r} \approx G^2_{K,L,r}(\varphi) := \frac{\sum_{\tau\in\mathcal{T}_{K,L,r}}|\tau||\nabla_\tau\varphi|^2}{\sum_{\tau\in\mathcal{T}_{K,L,r}}|\tau|}. \tag{3.2}$$

By this approach we find an approximation of the right-hand side of (3.1) consisting in replacing the surface integral by a simple quadrature, and the gradient projection by a finite difference expression

$$0 = \sum_{r\in\mathcal{R}}\sum_{L\sim K}\frac{|\overline{K}\cap\overline{L}\cap\Omega_r|}{|x_K-x_L|}\kappa_{0,r}F_r(T_{KL})G_{K,L,r}(\varphi)^{p_r-2}(\varphi_L-\varphi_K). \tag{3.3}$$

The same method for calculating the conductivity in the Joule heat term is combined with the technique proposed in [2] allowing to evaluate the Joule heating approximation by edge contributions: Gauss's theorem in the heat equation yields

$$0 = \sum_{L\sim K}\int_{\overline{K}\cap\overline{L}}\lambda(x)\nabla T\cdot\nu_{KL}\,\mathrm{da} + \int_K \eta(x)\kappa_0(x)F(x,T)|\nabla\varphi|^{p(x)}\,\mathrm{d}x, \tag{3.4}$$

and the suggested approach yields the approximation of the heat flow equation on K

$$\begin{aligned}0 =& \sum_{r\in\mathcal{R}}\sum_{L\sim K}\bigg(\frac{|\overline{K}\cap\overline{L}\cap\Omega_r|}{|x_K-x_L|}\lambda_r(T_L-T_K)\\ &+\frac{1}{2}\frac{|\overline{K}\cap\overline{L}\cap\Omega_r|}{|x_K-x_L|}\eta_r\kappa_{0,r}F_r(T_{KL})G_{K,L,r}(\varphi)^{p_r-2}(\varphi_L-\varphi_K)^2\bigg),\end{aligned} \tag{3.5}$$

where $T_{KL} = (T_K+T_L)/2$.

For Voronoi boxes $K\in\mathcal{V}$ with $\mathrm{mes}_{d-1}(\overline{K}\cap\overline{\partial\Omega}) > 0$ we additionally have to implement Dirichlet, no-flux or Robin boundary conditions, respectively,

$$w = w^D \text{ or } \quad -\nu\cdot(b\nabla w) = 0 \text{ or } \quad -\nu\cdot(b\nabla w) = e(w-w^D) \text{ on } \overline{K}\cap\overline{\Omega}_r\cap\overline{\partial\Omega}.$$

We write the flux over an outer face $\overline{K}\cap\overline{\Omega}_r\cap\overline{\partial\Omega}$ as $e_r(w_K - w_r^D)|\overline{K}\cap\overline{\Omega}_r\cap\overline{\partial\Omega}|$, where w_r^D corresponds to a mean of w^D on $\overline{K}\cap\overline{\Omega}_r\cap\overline{\partial\Omega}$, e_r is chosen very large to realize Dirichlet boundary values, e_r is set to zero for no-flux boundary conditions and it corresponds to a mean for e in case of Robin boundary conditions. Such that, according to (3.3) and (3.5) for all Voronoi boxes $K\in\mathcal{V}$ we have to solve

$$\begin{aligned}0 =& \sum_{r\in\mathcal{R}}\Big(\sum_{L\sim K}\frac{|\overline{K}\cap\overline{L}\cap\Omega_r|}{|x_K-x_L|}\kappa_{0,r}F_r(T_{KL})G_{K,L,r}(\varphi)^{p_r-2}(\varphi_L-\varphi_K)\\ &+ e_r(\varphi_K-\varphi_r^D)|\overline{K}\cap\overline{\Omega}_r\cap\overline{\partial\Omega}|\Big),\end{aligned} \tag{3.6}$$

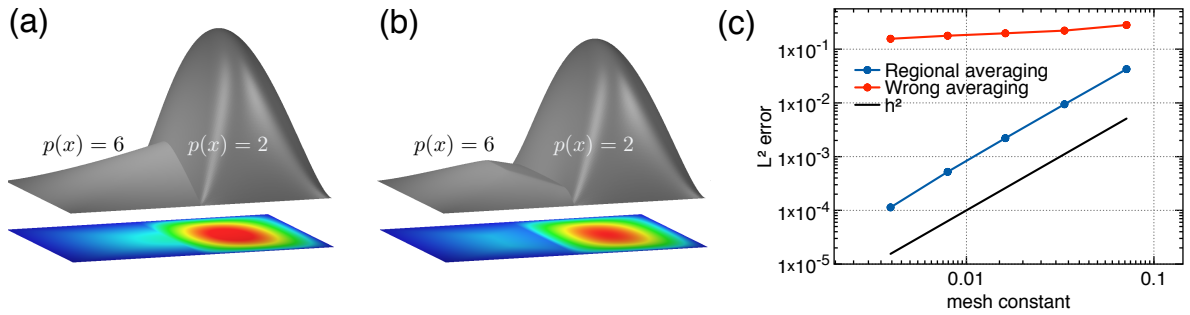

Figure 2: Discrete solutions of $p(x)$-Laplace equation (4.1) with constant right-hand side, homogeneous Dirichlet boundary conditions, and piecewise constant $p(x)$: (a) correct approximation, (b) wrong approximation with two local maxima due to gradient averaging ignoring the hetero interface, and (c) L^2 error of approximating solutions for correct and wrong averaging schemes

$$
\begin{aligned}
0 = \sum_{r\in\mathcal{R}} \sum_{L\sim K} \Bigg(& \frac{|\overline{K}\cap\overline{L}\cap\Omega_r|}{|x_K - x_L|}\lambda_r(T_L - T_K) \\
& + \frac{1}{2}\frac{|\overline{K}\cap\overline{L}\cap\Omega_r|}{|x_K - x_L|}\eta_r\kappa_{0,r}F_r(T_{KL})G_{K,L,r}(\varphi)^{p_r-2}(\varphi_L - \varphi_K)^2\Bigg) \\
& + \sum_{r\in\mathcal{R}} \gamma_r(T_K - T_a)|\overline{K}\cap\overline{\Omega}_r\cap\overline{\partial\Omega}|.
\end{aligned}
\tag{3.7}
$$

4 Numerical Tests for the $p(x)$-Laplacian

To justify our discretization ansatz for the gradient norm $|\nabla\varphi|$ in (3.2), we consider the two-dimensional test case for the $p(x)$-Laplacian

$$
-\nabla\cdot(|\nabla\varphi|^{p(x)-2}\nabla\varphi) = f \ \text{ in } \Omega, \quad \varphi = 0 \ \text{ on } \partial\Omega \tag{4.1}
$$

with fixed source term $f = 1$, where Ω is composed of two unit squares Ω_1 and Ω_2 being glued together at one edge and setting $p(x) = 6$ in Ω_1 and $p(x) = 2$ in Ω_2, respectively. The simulations in Fig. 2 illustrate the importance of taking care of the hetero interface when calculating the average of the gradient norm. An averaging over all simplices adjacent to a given edge regardless of the hetero region they belong to leads to an artificial diffusion along the hetero interface. We highlight the appearance of two local maxima (one centered in Ω_1 and one centered in Ω_2) in Fig. 2 (b). As shown in Fig. 2 (c), this effect cannot be diminished by grid refinement. Indeed, the L^2 error of the wrong averaging scheme with respect to the correct solution (Fig. 2 (a)) stays above a positive constant.

The validity of our approach (3.2) and the way it has been implemented (by (3.6) with right hand side $|K|$ and $\kappa_{0,r} = F_r(T_{KL}) = 1$, $\varphi_r^D = 0$, e_r large) hinges on the fact that all the measures $|\overline{K}\cap\overline{L}\cap\Omega_r|$ can be calculated from contributions from each simplex which at the hetero interfaces have to stay nonnegative. It is guaranteed by the boundary conforming Delaunay property of the underlying triangulation.

Table 1: Geometry and material parameters

Domain	p	E_{act} [eV]	κ_0 [1/(Ωm)]	λ [W/(mK)]	η	Thickness [nm]
Ω_{anode}	2.0	0.0	7.4×10^{-6}	1.0×10^{3}	1.0	9
Ω_1	4.07	0.325	7.7×10^{-8}	1.0×10^{3}	1.0	64
Ω_2	6.0	1.588	9.7×10^{-8}	1.0×10^{3}	0.8	20
Ω_3	4.7	0.2	2.1×10^{-7}	1.0×10^{3}	1.0	50

5 A Path Following Method for Simulating S-shaped Current-Voltage Relations

Our discretization scheme allows to simulate complicated three-dimensional OLED structures, see [6]. As an example we consider a crossbar OLED stack depicted in Fig. 1 (left), given by two stacked cuboids Ω_{anode} and Ω_{org}. The upper one, Ω_{anode}, representing the optically transparent anode is overlapping to the left and electrically contacted only on the left side Γ_+. The lower one, Ω_{org}, consisting of the organic semiconducting layers Ω_1, Ω_2, and Ω_3 realizes the actual OLED structure with an active area of $2\,\text{mm} \times 2\,\text{mm}$, see Fig. 1 (left). The organic material is contacted by a metal layer. Due to the high conductivity of this layer we assume that the potential is constant here and neglect the metal layer entirely in the simulations by prescribing Dirichlet boundary conditions on the bottom Γ_- of Ω_3.

On Γ_- the potential is set to zero and on Γ_+ to the (spatially constant) externally applied voltage V. We determine the current-voltage relation of the OLED stack (which can be S-shaped) by calculating the current over Γ_+. Then, the Dirichlet boundary is given by $\Gamma^D = \Gamma_+ \cup \Gamma_-$. The ambient temperature is fixed to $293\,\text{K}$, the other essential parameters for the simulation are collected in Table 1.

With the equations (3.6) and (3.7) for all Voronoi boxes $K \in \mathcal{V}$ we arrive at a system of $2m$ coupled nonlinear algebraic equations for $u = (\varphi_K, T_K)_{K\in\mathcal{V}}$ of the form

$$g(u, V) = 0, \quad g : \mathbb{R}^{2m} \times \mathbb{R} \to \mathbb{R}^{2m}.$$

To trace a solution branch, starting from a solution (u_0, V_0) of $g(u, V) = 0$ we use a predictor-corrector method [10] adapted to PDE calculations as proposed in [1]. The prediction is obtained by moving forward a step along the tangent t to the branch. First we solve $g_{u,V}(u_0, V_0)t = 0, t \in \mathbb{R}^{2m+1}$. To ensure that t points in the forward direction with respect to the tangent t_0 of the last point, we demand $t_0 \cdot t > 0$. In other words, we have to solve

$$\begin{pmatrix} g_{u,V}(u_0, V_0) \\ t_0 \end{pmatrix} t = \begin{pmatrix} 0 \\ 1 \end{pmatrix}.$$

Next, we normalize t such that $\|t\| = 1$. Our predictor (u^*, V^*) now is choosen as

$$\begin{pmatrix} u^* \\ V^* \end{pmatrix} = \begin{pmatrix} u_0 \\ V_0 \end{pmatrix} + \frac{\Delta L}{\|t\|_*} t, \quad \text{where } \|t\|_*^2 = \frac{1}{2m} \sum_{i=1}^{2m} t_i^2 + t_{2m+1}^2$$

ensures that a step along the branch gives similar proportion to the unknowns and to the parameter, and, by construction, $\|u^* - u_0, V^* - V_0\|_* = \Delta L$. The corrector step consists in solving the nonlinear

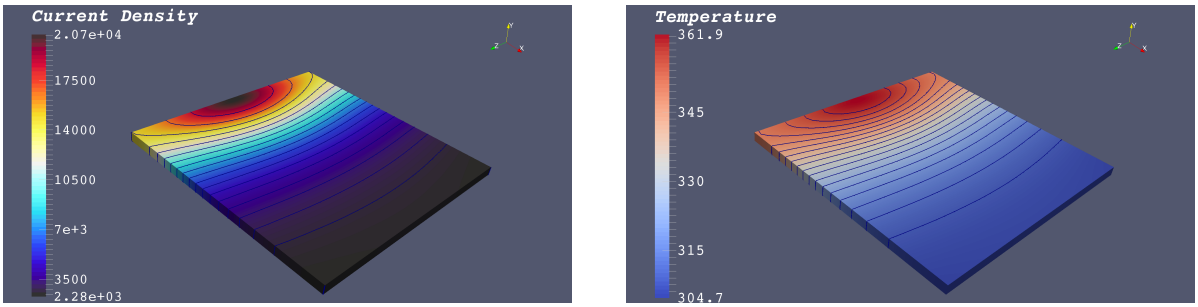

Figure 3: Simulated current density $[\mathrm{A}/\mathrm{m}^2]$ (left) and temperature distribution [K] (right) in horizontal cross section through the middle of the organic emitter layer at an applied voltage of $6.5\,\mathrm{V}$

system

$$\begin{pmatrix} g(u,V) \\ \|u-u_0, V-V_0\|_*^2 - (\Delta L)^2 \end{pmatrix} = 0$$

by Newton's method, where the calculated prediction (u^*, V^*) is used as starting value. If Newton's method does not converge, meaning that the predictor is too far from the desired solution, the step size ΔL (related to the arc length parameter) is locally reduced until the method is convergent. The convergent Newton procedure yields the next point (u_1, V_1) on the solution branch with a distance of ΔL to (u_0, V_0).

Fig. 3 contains the simulated current density and the temperature distribution in a horizontal cross section in the emitting layer of the OLED material for an applied voltage of $6.5\,\mathrm{V}$. Have in mind that the temperature and current density maxima appear at the side where the anode voltage is applied. Fig. 1 (right) shows simulated S-shaped current voltage relations for test structures with different thermal outcoupling regimes realized by varying heat transfer coefficients γ in (2.2).

Acknowledgement

A.G. and M.L. gratefully acknowledge the funding received via Research Center MATHEON supported by ECMath in project D-SE2.

References

[1] Bloch, J., Fuhrmann, J., Gärtner, K.: Bifurcation analysis of nonlinear systems of PDE's. unpublished report

[2] Bradji, A., Herbin, R.: Discretization of coupled heat and electrical diffusion problems by finite-element and finite-volume methods. IMA J. Numer. Anal. **28**(3), 469–495 (2008)

[3] Bulíček, M., Glitzky, A., Liero, M.: Systems describing electrothermal effects with $p(x)$-Laplace like structure for discontinuous variable exponents. SIAM J. Math. Analysis **48**, 3496–3514 (2016)

[4] Bulíček, M., Glitzky, A., Liero, M.: Thermistor systems of $p(x)$-Laplace-type with discontinuous exponents via entropy solutions. to appear in DCDS-S (WIAS Preprint 2247 (2016))

[5] Eymard, R., Gallouët, T., Herbin, R.: Discretization of heterogeneous and anisotropic diffusion problems on general nonconforming meshes. IMA J. Numer. Anal. **30**, 1009–1043 (2010)

[6] Fischer, A., Koprucki, T., Gärtner, K., Brückner, J., Lüssem, B., Leo, K., Glitzky, A., Scholz, R.: Feel the heat: Nonlinear electrothermal feedback in organic LEDs. Adv. Funct. Mater. **24**, 3367–3374 (2014)

[7] Fischer, A., Pahner, P., Lüssem, B., Leo, K., Scholz, R., Koprucki, T., Gärtner, K., Glitzky, A.: Self-heating, bistability, and thermal switching in organic semiconductors. Phys. Rev. Lett. **110**, 126,601/1–126,601/5 (2013)

[8] Glitzky, A., Liero, M.: Analysis of $p(x)$-Laplace thermistor models describing the electrothermal behavior of organic semiconductor devices. Nonlinear Anal. Real World Appl. **34**, 536–562 (2017)

[9] Liero, M., Koprucki, T., Fischer, A., Scholz, R., Glitzky, A.: p-Laplace thermistor modeling of electrothermal feedback in organic semiconductor devices. Z. Angew. Math. Phys. **66**, 2957–2977 (2015)

[10] Seydel, R.: Practical bifurcation and stability analysis. Springer (1994)

[11] Si, H., Gärtner, K., Fuhrmann, J.: Boundary conforming Delaunay mesh generation. Computational Mathematics and Mathematical Physics **50**(1), 38–53 (2010)